

Determination of the Spin of New Resonances in Electroweak Gauge Boson Pair Production at the LHC

O. J. P. Éboli*

Instituto de Física, Universidade de São Paulo, São Paulo – SP, Brazil.

Chee Sheng Fong

C.N. Yang Institute for Theoretical Physics, SUNY at Stony Brook, Stony Brook, NY 11794-3840, USA

J. Gonzalez-Fraile†

*Departament d'Estructura i Constituents de la Matèria and ICC-UB,
Universitat de Barcelona, 647 Diagonal, E-08028 Barcelona, Spain*

M. C. Gonzalez-Garcia‡

*C.N. Yang Institute for Theoretical Physics, SUNY at Stony Brook, Stony Brook, NY 11794-3840, USA and
Institució Catalana de Recerca i Estudis Avançats (ICREA),
Departament d'Estructura i Constituents de la Matèria,
Universitat de Barcelona, 647 Diagonal, E-08028 Barcelona, Spain*

The appearance of spin-1 resonances associated to the electroweak symmetry breaking (EWSB) sector is expected in many extensions of the Standard Model. We analyze the CERN Large Hadron Collider potential to probe the spin of possible new charged and neutral vector resonances through the purely leptonic processes $pp \rightarrow Z' \rightarrow \ell^+ \ell'^- \cancel{E}_T$, and $pp \rightarrow W' \rightarrow \ell'^{\pm} \ell^+ \ell^- \cancel{E}_T$, with $\ell, \ell' = e$ or μ . We perform a model independent analysis and demonstrate that the spin of the new states can be determined with 99% CL in a large fraction of the parameter space where these resonances can be observed with 100 fb^{-1} . We show that the best sensitivity to the spin is obtained by directly studying correlations between the final state leptons, without the need of reconstructing the events in their center-of-mass frames.

PACS numbers: 12.60.Fr, 14.70.Pw

I. INTRODUCTION

One of the prime objectives of the CERN Large Hadron Collider (LHC) is to probe directly the EWSB sector. The analysis of partial wave unitarity of longitudinal weak boson scattering guarantees that there should exist a new state at the TeV scale or that this process becomes strongly interacting at high energies [1, 2]. In several extensions of the Standard Model (SM) the new resonances associated to the unitarity restoration are expected to have spin 1. For instance, in Higgsless models a tower of spin-1 particles is responsible for cutting off the growth of the electroweak gauge boson scattering amplitude without the presence of any scalar (Higgs) field [3]. Another attractive possibility is that the electroweak symmetry breaking is associated to a new strongly interacting sector [4]. These models also exhibit new vector states that contribute to the unitarization of the weak gauge boson scattering [5].

Thus, a common feature of many EWSB scenarios, as the ones above mentioned, is the existence of new vector resonances, Z' and W' , that couple to $W^+ W^-$ and $W^\pm Z$ pairs respectively. But, generically, their properties, such as mass, width, and couplings to SM particles, are model dependent. In this respect, the *model independent* channels for detection of such spin-1 resonances would be their production via weak boson fusion (WBF) or its associated production with an electroweak gauge boson, since both processes only involve their couplings to electroweak gauge bosons. Unfortunately for a Z' these signals are unobservable in a clean purely leptonic channel at LHC even with increased luminosity [6–8], while W' can be observed in the WBF $W^\pm Z \rightarrow W^\pm Z$ elastic scattering [6, 7]. Once a clear signal of the charged resonance is observed in the above channels, it is mandatory to study its spin to confirm that the new state is indeed a vector particle. Much work has been devoted in the literature over the last years to this issue [9–11]. For this purpose the WBF process can be used to determine the spin of a W' resonance at LHC, however, only for relatively light resonances and with the assumption of increased luminosity [7].

Alternatively the new spin-1 states can also be directly produced in pp collisions via its coupling to light quarks

*Electronic address: eboli@fma.if.usp.br

†Electronic address: fraile@ecm.ub.es

‡Electronic address: concha@insti.physics.sunysb.edu

and in order to establish that such new vector bosons are indeed associated with EWSB one should analyze processes in which the new spin-1 decays into electroweak gauge boson [12]. In this work we investigate the LHC potential to determine the spin of a new resonance responsible for the unitarization of weak boson scattering amplitude by the study of the processes

$$\begin{aligned} pp &\rightarrow Z' \rightarrow W^+W^- \rightarrow \ell^+\ell'^-\cancel{E}_T \\ pp &\rightarrow W' \rightarrow W^\pm Z \rightarrow \ell^+\ell^-\ell'^\pm\cancel{E}_T \end{aligned} \quad (1)$$

Instead of assuming a specific model for EWSB we express our results as a function of the relevant couplings of the new neutral (charged) resonance to light quarks and W^+W^- ($W^\pm Z$) pairs, and of its width and mass. The spin assignment of the new resonances is obtained from the spin correlation between the final state leptons, contrasting the expected results for spin-1 and spin-0 new states, *i.e.* we work in the framework commonly used to analyze the spin of supersymmetric particles [9, 10]. We also study the angular distribution of the produced EW gauge bosons in the V' center of mass. In order to do so one needs to reconstruct the neutrino momenta for the processes (1). For the topology $\ell^+\ell^-\ell'^\pm\cancel{E}_T$, associated with the W' production, the neutrino longitudinal momentum was obtained requiring that it is compatible with the production of an on-shell W . To reconstruct the momenta of the two neutrinos coming from Z' production we used the M_{T2} assisted on-shell (MAOS) reconstruction [13]. We show that the best sensitivity is obtained by directly studying the final state leptons and we quantify the correlated ranges of V' couplings, masses, widths and collider luminosity for which the spin of the resonance can be established at a given CL.

II. FRAMEWORK

In order to study the processes (1) we must know the couplings of the new resonance to light quarks and electroweak gauge bosons, as well as its mass and width. Here we will consider that these are free parameter without restricting ourselves to any specific model. However, for the sake of concreteness we assume that the couplings of the Z' and the W' to the light quarks and to gauge bosons have the same Lorentz structure as those of the SM, as suggested by the Higgsless models, but with arbitrary strength. Furthermore, we vetoed the Z' coupling to ZZ pairs as it happens in this class of models.

The partial wave amplitude for the process $W^+W^- \rightarrow W^+W^-$ is saturated by the exchange of a Z' provided its coupling to electroweak gauge bosons satisfies [6]

$$g_{Z'WW_{max}} = g_{ZWW} \frac{M_Z}{\sqrt{3}M_{Z'}} \quad (2)$$

with $g_{ZWW} = g c_W$ being the strength of the SM triple gauge boson coupling. Here g stands for the $SU(2)_L$

coupling constant and c_W is the cosine of the weak mixing angle.

Analogously, a charged vector resonance saturates unitarity of the scattering $W^\pm Z \rightarrow W^\pm Z$ for [6]

$$g_{W'WZ_{max}} = g_{ZWW} \frac{M_Z^2}{\sqrt{3}M_{W'}M_W} \quad (3)$$

In what follows we use $g_{W'WZ_{max}}$ and $g_{Z'WW_{max}}$ simply as convenient normalizations for the coupling of the spin-1 resonance to SM gauge bosons.

The width of the new spin-1 resonances receives contributions from its decay to light quarks and electroweak gauge boson pairs, as well as into other states, like t or b . Therefore, in this work we treat the Z' and W' widths as a free parameters. In this approach, for each final state the analysis depends on three parameters: the mass of the resonance, $M_{V'}$; its width, $\Gamma_{V'}$; and the product of its couplings to light quarks and to SM gauge bosons, $g_{V'q\bar{q}} g_{V'WV}$. These parameters are only subject to the constraint that for a given value of product of the couplings of the new resonance and of its mass, there is lower bound on its width that reads [12]

$$\Gamma_{Z'} > 0.27 \text{ GeV} \left(\frac{g_{Z'q\bar{q}}}{g_{Zq\bar{q}}} \right) \left(\frac{g_{Z'WW}}{g_{ZWW_{max}}} \right) \left(\frac{M_{Z'}}{M_Z} \right)^2 \quad (4)$$

$$\Gamma_{W'} > 0.40 \text{ GeV} \left(\frac{g_{W'q\bar{q}}}{g_{Wq\bar{q}}} \right) \left(\frac{g_{W'WZ}}{g_{WZ_{max}}} \right) \left(\frac{M_{W'}}{M_W} \right)^2 \quad (5)$$

where $g_{Zq\bar{q}} = g/c_W$ and $g_{Wq\bar{q}'} = g/\sqrt{2}$.

Within our approach we can express the cross section for the processes (1) as

$$\begin{aligned} \sigma_{\text{tot}} = & \sigma_{SM} + \left(\frac{g_{V'q\bar{q}}}{g_{Vq\bar{q}}} \frac{g_{V'WV}}{g_{V'WW_{max}}} \right) \sigma_{int}(M_{V'}, \Gamma_{V'}) \\ & + \left(\frac{g_{V'q\bar{q}}}{g_{Vq\bar{q}}} \frac{g_{V'WV}}{g_{V'WW_{max}}} \right)^2 \sigma_{V'}(M_{V'}, \Gamma_{V'}) \end{aligned} \quad (6)$$

where the Standard Model, interference and new resonance contributions are labeled SM , int and V' respectively. Moreover, for $V' = Z'$, $g_{V'WV} \equiv g_{Z'WW}$ and $g_{V'q\bar{q}} \equiv g_{Z'q\bar{q}}$ while for $V' = W'$, $g_{V'WV} \equiv g_{W'WZ}$ and $g_{V'q\bar{q}} \equiv g_{W'q\bar{q}}$.

By construction our analysis applies to any V' whose couplings to the SM u- and d-quarks and to the SM gauge bosons are a simple rescaling of the W or Z couplings. Conversely the analysis renders limited information on the underlying physics associated to the new resonances unless combined with information from other channels for the observation of these states. For instance, the processes (1) give information on the couplings to light quark pairs and electroweak gauge bosons. Analyzing the weak boson fusion production of these particles allow us to disentangle the couplings to gauge bosons and quarks. Certainly additional information can be gathered by studying further channel like the associated production with a gauge boson or the new resonance decay into leptons.

We perform our analyses at the parton level, keeping the full helicity structure of the amplitude. This is achieved using the package MADGRAPH [14] modified to include the new vector states and their couplings. In our calculations we use CTEQ6L parton distribution functions [15] with renormalization and factorization scales $\mu_F^0 = \mu_R^0 = \sqrt{(p_T^{\ell+2} + p_T^{\ell-2})/2}$ where $p_T^{\ell\pm}$ is the transverse momentum of the two charged leptons in the Z' decay or of the two different flavor opposite sign leptons in the W' decay. For the case of W' decaying into three equal flavor leptons we choose the two opposite sign leptons whose invariant mass is not compatible with being the decay products of a Z . Furthermore, we simulate experimental resolutions by smearing the energies, but not directions, of all final state leptons with a Gaussian error given by a resolution $\Delta E/E = 0.1/\sqrt{E} \oplus 0.01(E \text{ in GeV})$. We also consider a lepton detection efficiency of $\epsilon^\ell = 0.9$.

III. W' SPIN DETERMINATION

We analyzed W' production in the channel

$$pp \rightarrow W' \rightarrow ZW^\pm \rightarrow \ell^+ \ell^- \ell'^\pm \cancel{E}_T$$

with $\ell = e$ or μ . The main SM backgrounds are the production of electroweak gauge boson pairs $W^\pm Z$ and ZZ with its subsequent leptonic decay. In the ZZ production one of the final state leptons must evade detection. The SM production of top quarks can also lead to trilepton final states, however, this process is rather suppressed since one of the isolated leptons must originate from the semi-leptonic decay of a b quark.

The starting cuts are meant to ensure the detection and isolation of the final leptons plus a minimum transverse momentum:

$$|\eta_\ell| < 2.5, \Delta R_{\ell\ell} > 0.2, p_T^\ell > 10 \text{ GeV and } \cancel{E}_T > 10 \text{ GeV} \quad (7)$$

Next, we look for a same flavor opposite charge lepton pair that is compatible with a Z , *i.e.*

$$|M_{\ell+\ell-} - M_Z| < 20 \text{ GeV}. \quad (8)$$

We also demand in the search for the resonance that the hardest observed lepton has transverse momentum in excess of 120 GeV in order to tame the SM backgrounds.

In this process the neutrino momentum can be reconstructed up to a two-fold ambiguity: its transverse momentum can be directly obtained from momentum conservation in the transverse directions while its longitudinal component can be inferred by requiring that $(p^\nu + p^\ell)^2 = M_W^2$, which leads to

$$p_L^\nu = \frac{1}{2p_T^{\ell^2}} \left\{ [M_W^2 + 2(p_T^{\ell^2} \cdot \cancel{p}_T)] p_L^\ell \pm \sqrt{[M_W^2 + 2(p_T^{\ell^2} \cdot \cancel{p}_T)]^2 |\vec{p}^{\ell^2}|^2 - 4(p_T^{\ell^2} E^\ell \cancel{E}_T)^2} \right\} \quad (9)$$

where p^ℓ is the four-momentum of the charged lepton not associated to the Z . With the two values of the reconstructed neutrino momenta we obtain two possible solutions for the invariant mass of the $\ell\ell\nu$ system. In order to enhance the signal and reduce the SM backgrounds we require that the final state is compatible with a W' production of a given mass,

$$|M_{\text{rec}}^{\text{min}} - M_{W'}| < \delta. \quad (10)$$

where $M_{\text{rec}}^{\text{min}}$ is the smaller of the two solutions. In our analysis we consider three reference W' masses 500 GeV, 1 TeV, and 1.5 TeV, and we took $\delta = 50, 100$, and 200 GeV for the three cases, respectively.

We show in Fig. 1 (upper panel) the values of $\sigma_{W'}(M_{W'}, \Gamma_{W'})$ and σ_{SM} (which after cut (10) is also a function of $M_{W'}$) at $\sqrt{s} = 14$ TeV. Once the cuts described above are imposed the interference term is negligible for all values of W' mass and widths considered. As seen from this figure the SM backgrounds diminish as the new state becomes heavier, as expected, and the signal cross section deteriorates as the width of the resonance grows. Moreover, this channel presents a small SM background due to the reduced leptonic branching ratio of the electroweak gauge bosons. For the sake of completeness we depict in Fig. 1 (lower panel) the region of the parameter space where the LHC will be able to observe a W' with at least 5σ significance level for an integrated luminosity of 100 fb^{-1} . For this luminosity the number of background events is large enough for Gaussian statistics to hold for $M_{W'} = 500$ and 1000 GeV and we impose $N_{W'} \geq 5\sqrt{N_{SM}}$ where $N_{W',SM} = \mathcal{L} \times \sigma_{W',SM} \times (\epsilon^\ell)^3$. For $M_{W'} = 1500$ GeV the number of expected background events is $N_{SM} = 9.8$ and we adopt the corresponding 5σ observability bound for Poisson statistics in the presence of this background, *i.e.* $N_{W'} > 18$. As expected larger couplings are required for the observation as the resonances broaden. The upper bounds on the discovery region are due to the constraint (5) on the couplings for a given W' width. As a final remark, with a reduced integrated luminosity of 10 fb^{-1} the lower line of minimum coupling constant product needed for discovery is increased by a factor $\simeq 3$, however, a sizable fraction of the parameter space can still be probed.

It is interesting to compare the results depicted in the lower panel of Fig. 1 with the direct searches for a W' performed so far. A comparison of these searches, unfortunately, is model dependent since the experimental analyses relied on a specific model. For instance, they used the direct interactions of the new W' states with leptons, which is not present in our parameterization. The only exception is the CDF Collaboration search for new WW and WZ resonances in $p\bar{p} \rightarrow e^\pm jj \cancel{E}_T$ [16]. This work excludes a narrow 500 GeV W' at 95% CL provided

$$\left(\frac{g_{W'q\bar{q}}}{g/\sqrt{2}} \times \frac{g_{W'WZ}}{g_{W'WZ_{max}}} \right) \gtrsim 0.21$$

This implies that a small left corner of Fig. 1 is probably already excluded.

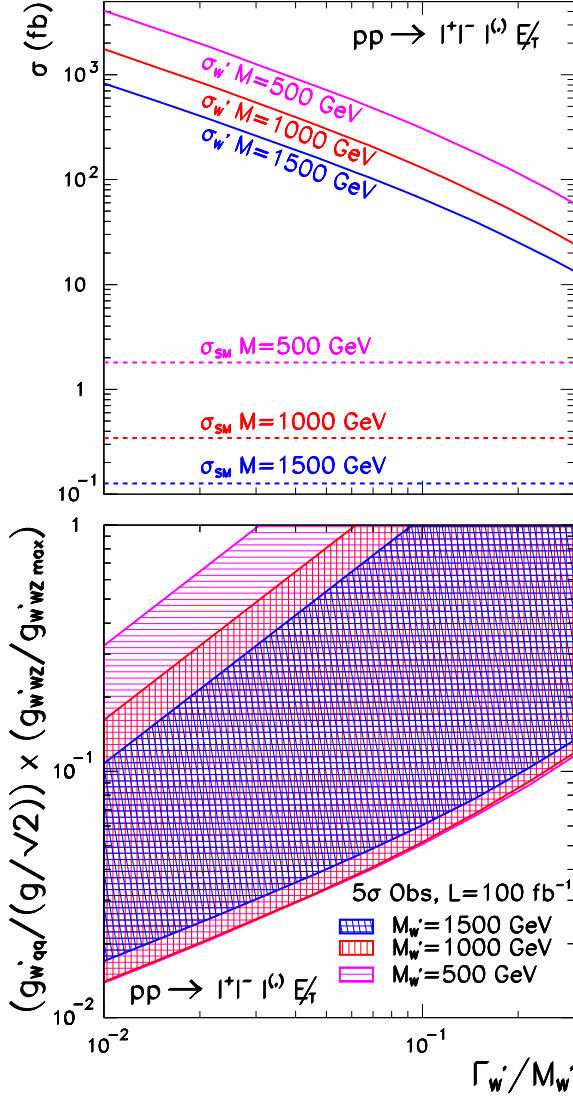


FIG. 1: **Upper panel:** signal and background cross sections for the $\ell^+\ell^-\ell'^\pm\cancel{E}_T$ final state for all possible lepton combinations without including lepton detection efficiencies. **Lower panel:** the filled regions are the ranges of the parameters for observation of a W' with mass $M_{W'} = 0.5, 1, \text{ and } 1.5$ TeV with at least 5σ significance in the reaction $pp \rightarrow W' \rightarrow ZW^\pm \rightarrow \ell^+\ell^-\ell'^\pm\cancel{E}_T$ and an integrated luminosity of 100 fb^{-1} .

In previous studies [9], it has been shown that a convenient variable for contrasting the production of particles with different spin is

$$\cos\theta_{\ell\ell}^* \equiv \tanh\left(\frac{\Delta\eta_{\ell\ell}}{2}\right), \quad (11)$$

where $\Delta\eta_{\ell\ell}$ is the rapidity difference between the same charge leptons. This quantity has the advantage of being invariant under longitudinal boosts. We present in the

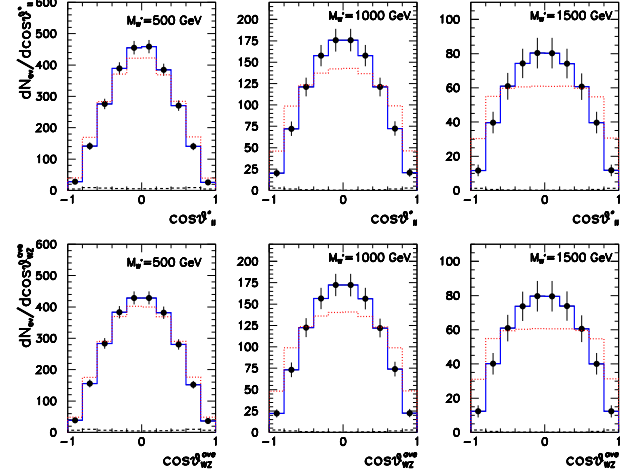


FIG. 2: $\cos\theta_{\ell\ell}^*$ (upper panels) and $\cos\theta_{WZ}^{ave}$ (lower panels) distributions for the production of the charged vector resonance W' (solid blue line with error bars), and the production of a charged scalar resonance (dotted red line). The results are shown for $\Gamma_{W'} = 0.05M_{W'}$ and $\left(\frac{g_{W'q\ell}}{g_{W'q\ell}} - \frac{g_{W'WZ}}{g_{W'WZ}^{max}}\right) = 0.3$. The SM contribution (barely visible) is the dashed black line at the bottom. Here we assumed an integrated luminosity of 100 fb^{-1} .

upper panels of Fig. 2 the $\cos\theta_{\ell\ell}^*$ spectrum for the production of spin-0 and spin-1 resonances and our three reference masses. In order to compare the spin-0 and spin-1 angular correlations we assumed that the production cross section of the spin-0 particles is equal to the one for spin-1 particles, and we imposed that the scalar and vector resonances have the same mass and width. As we can see, the $\cos\theta_{\ell\ell}^*$ distribution for W' vector production exhibits a maximum at $\cos\theta_{\ell\ell}^* = 0$, as expected. In principle this spectrum should be flat in the production of scalars, however, the acceptance cuts, especially $|\eta_\ell| < 2.5$, distort this spectrum, which reduces the discriminating power for light resonances.

The extraction of the final state neutrino momentum allow us to reconstruct angular correlations in the WZ center-of-mass frame. Therefore, we also study the spin correlations using the reconstructed Z polar angle (θ_{WZ}) distribution evaluated in the WZ center-of-mass frame. Since there is a two-fold ambiguity in this reconstruction, we consider the average of the two resulting distributions in our analysis. As shown in Ref. [7] the angular distribution of the reconstructed $\cos\theta_{WZ}$ for the reconstruction yielding minimum (maximum) WZ invariant mass, is peaked (has a valley) around zero when compared to the true θ_{WZ} but the average of the two has a very similar distribution to the true one. We plot in the lower panels of Fig. 2 the $\cos\theta_{WZ}^{ave}$ spectrum for the production of spin-0 and spin-1 resonances and our three reference masses. Comparing the distributions in the two angular variables $\cos\theta_{\ell\ell}^*$ and $\cos\theta_{WZ}^{ave}$ we learn that they are very

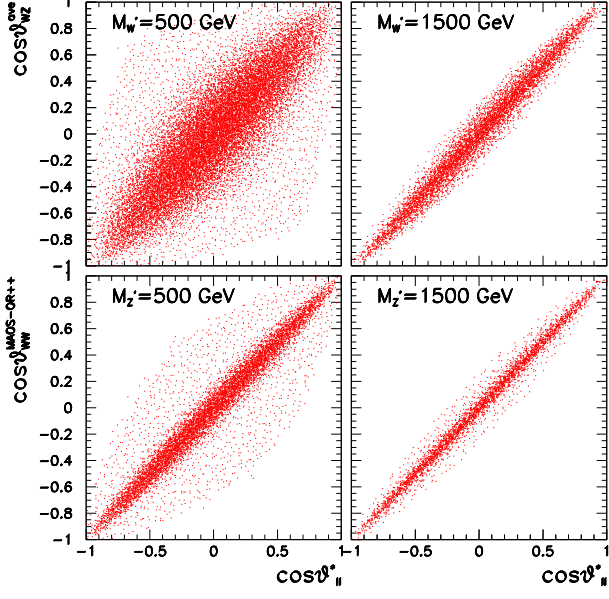


FIG. 3: The upper panels contain the $\cos \theta_{\ell\ell}^* \otimes \cos \theta_{WZ}^{ave}$ spectrum for W' and $M_{W'} = 0.5$ TeV (upper left panel) and 1.5 TeV (upper right panel) where $\cos \theta_{WZ}^{ave}$ is the average of the two possible solutions. The lower panels depict the $\cos \theta_{\ell\ell}^* \otimes \cos \theta_{WW}^{MAOS-OR++}$ spectrum for Z' and $M_{Z'} = 0.5$ TeV (lower left panel) and 1.5 TeV (lower right panel).

similar. Indeed they happen to be strongly correlated as shown in the upper panels of Fig. 3, where we plot the $\cos \theta_{\ell\ell}^* \otimes \cos \theta_{WZ}^{ave}$ spectrum for $M_{W'} = 0.5$ TeV (upper left panel) and 1.5 TeV (upper right panel). The figure is for $\Gamma_{W'} = 0.05 M_{W'}$, but the results are very insensitive to the precise value of the width. It is clear from Fig. 3 that there is a strong correlation between $\cos \theta_{\ell\ell}^*$ and $\cos \theta_{WZ}^{ave}$, which is somehow unforeseen given the definitions of both variables and the different behaviours of the $\cos \theta_{WZ}^{max}$ and $\cos \theta_{WZ}^{min}$ distributions. As expected the correlation gets stronger as the W' mass increases since heavier resonances decay into more energetic electroweak gauge bosons and consequently the final state leptons have the tendency to follow the direction of the parent W or Z .

Taking into account the correlation between $\cos \theta_{\ell\ell}^*$ and $\cos \theta_{WZ}^{ave}$, it is expected that both kinematical variables have a comparable spin discriminating power. In fact, this is the case except for $M_{W'} = 500$ GeV, where $\cos \theta_{WZ}^{ave}$ performs slightly worse. Furthermore we should keep in mind that larger systematic uncertainties are expected in the reconstruction of θ_{WZ} associated with the understanding and calibration of the detector due to the measurement of missing transverse momentum.

In order to quantify the parameter space region for which a positive discrimination between spin-0 and spin-

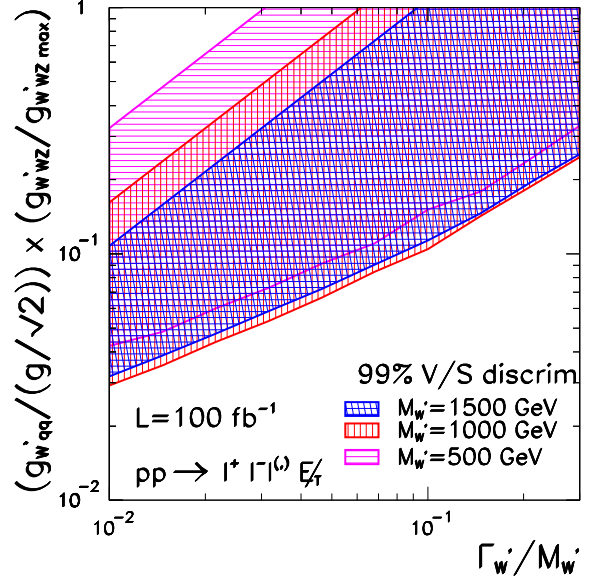


FIG. 4: Parameter space region where the W' spin can be determined with 99% CL using the asymmetry $A_{\ell\ell}$ for an integrated luminosity of 100 fb^{-1} .

1 resonances is possible we construct the asymmetry

$$A_{\ell\ell} = \frac{\sigma(|\cos \theta_{\ell\ell}^*| < 0.5) - \sigma(|\cos \theta_{\ell\ell}^*| > 0.5)}{\sigma(|\cos \theta_{\ell\ell}^*| < 0.5) + \sigma(|\cos \theta_{\ell\ell}^*| > 0.5)}. \quad (12)$$

Notice that this observable eliminates possible normalization systematics in the angular distributions.

Fig. 4 displays the region in the parameter space where the W' spin can be established with 99% CL using $A_{\ell\ell}$ for an integrated luminosity of $\mathcal{L}=100 \text{ fb}^{-1}$ at the LHC. This result was obtained taking into account only the statistical errors and assuming that the observed distribution follows that of a vector resonance. With this hypothesis the 99% CL spin discrimination condition reads:

$$|A_{\ell\ell}^V - A_{\ell\ell}^S| \geq 2.58 \sigma_{A_{\ell\ell}^V} = 2.58 \frac{\sqrt{1 - A_{\ell\ell}^{V^2}}}{\sqrt{N_{\text{tot}}}} \quad (13)$$

where $\sigma_{A_{\ell\ell}^V}$ is the expected statistical error of the variable $A_{\ell\ell}^V$ and $N_{\text{tot}} = \mathcal{L} \times \sigma_{\text{tot}} \times (\epsilon^\ell)^3$ with σ_{tot} in Eq. (6). In writing Eq. (13) we implicitly assume that for the 99% spin determination the number of events N_{tot} is always large enough for Gaussian statistics to hold. We verify that this is the case even for the smallest couplings for which 99% CL spin determination is possible and therefore the procedure is consistent.

Comparing Figs. 4 and 1 we see that the minimum couplings necessary to determine the spin at 99% CL for this integrated luminosity is a factor of an order of 2 larger than the minimum couplings needed for its discovery.

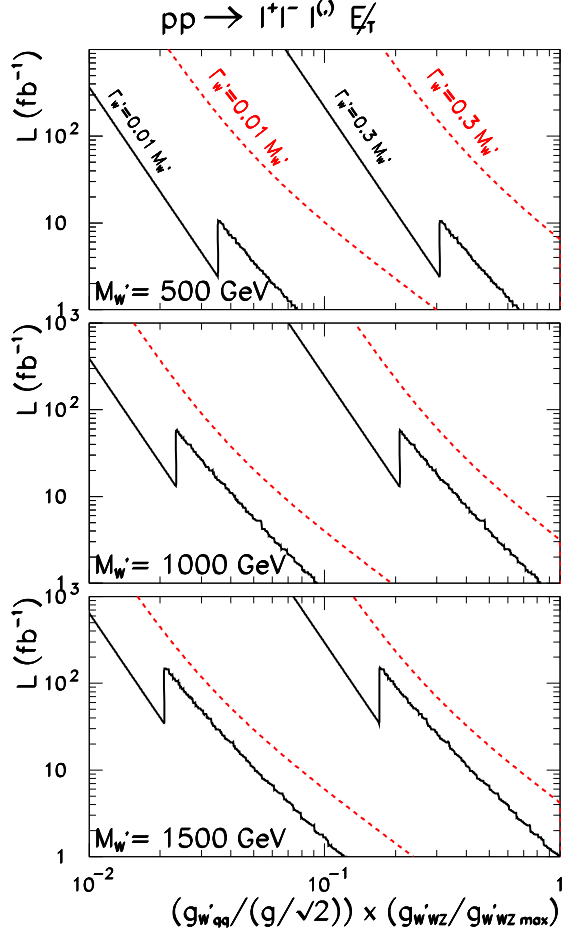


FIG. 5: The solid (dashed) lines stand for integrated luminosity required for the discovery (99% CL spin determination) as a function of the vector resonance couplings. We present the results for three masses and two widths: $\Gamma_{W'} = 0.01M_{W'}$ and $\Gamma_{W'} = 0.3M_{W'}$. See text for detailed information on the statistics used in this figure.

Moreover, as seen in Fig. 2, the acceptance cuts modify more drastically the distributions for lighter W' masses, and consequently, the discrimination between spin-0 and spin-1 requires a larger statistics, reflected in larger couplings and production cross sections. Notwithstanding, the LHC will be able to successfully unravel the spin of a possible new state with 99% CL in a large fraction of the parameter space of discovery.

In order to address the potential of the LHC from earlier runs or with upgraded luminosity, but still at 14 TeV, we quantify the luminosity requirement for discovery and spin determination of the resonance as a function of its parameters. Fig. 5 depicts the integrated luminosity needed for a 5σ discovery (solid lines) and 99% CL spin determination based on (13) (dashed lines) as a function of its couplings for our three reference masses and two widths ($\Gamma_{W'} = 0.01M_{W'}$ and $\Gamma_{W'} = 0.3M_{W'}$). The

discovery requirements were obtained using Poisson or Gaussian statistics depending on whether the expected number of SM events was smaller or larger than 15 and the changing from one to the other determines the discontinuity in the corresponding lines. For the 99% CL spin determination the number of expected events is always large enough for Gaussian statistics to hold. As we can see from Fig. 5, an earlier discovery, *e.g.* with 10 fb^{-1} , is possible even for rather weakly coupled W' . Although the W' spin determination requires larger couplings it can also be carried out in a sizable region of the parameter space in earlier runs.

IV. Z' SPIN DETERMINATION

We study the Z' spin through the reaction

$$pp \rightarrow Z' \rightarrow W^+W^- \rightarrow \ell^+\ell'^-\cancel{E}_T.$$

The main SM backgrounds to this process are the production of W^+W^- with its subsequent leptonic decay, the ZZ production with one Z decaying into charged leptons and the other decaying invisibly or with both Z decaying into charged leptons two of which escape undetected. Additional backgrounds are provided by the SM production of $t\bar{t}$ pairs with both top quarks decaying semileptonically as well as the $\tau^+\tau^-$ production with both τ 's decaying leptonically.

We begin our analysis requiring two final state leptons with opposite charge and applying acceptance and isolation cuts on them

$$|\eta_\ell| < 2.5, \quad \Delta R_{\ell\ell} > 0.2 \quad \text{and} \quad p_T^\ell > 50 \text{ GeV} \quad (14)$$

The presence of two neutrinos in the final state renders impossible the complete reconstruction of the event. A possible variable to characterize the signal is the transverse invariant mass,

$$M_T^{WW} = \left[\left(\sqrt{(p_T^{\ell^+\ell'^-})^2 + m_{\ell^+\ell'^-}^2} + \sqrt{\cancel{p}_T^2 + m_{\ell^+\ell'^-}^2} \right)^2 - (\vec{p}_T^{\ell^+\ell'^-} + \vec{\cancel{p}}_T)^2 \right]^{1/2} \quad (15)$$

where $\vec{\cancel{p}}_T$ is the missing transverse momentum vector, $\vec{p}_T^{\ell^+\ell'^-}$ is the transverse momentum of the pair $\ell^+\ell'^-$ and $m_{\ell^+\ell'^-}$ is the $\ell^+\ell'^-$ invariant mass.

Alternatively we attempt to reconstruct the WW invariant mass by estimating the momenta of the two escaping neutrinos produced using the M_{T2} Assisted on-Shell (MAOS) reconstruction [13]. For $W^+(p_1 + p_2)W^-(k_1 + k_2) \rightarrow \ell^+(p_1)\nu(p_2)\ell^-(k_1)\nu(k_2)$ the variable M_{T2} is defined as [17]

$$M_{T2} \equiv \min_{\mathbf{p}_{2T} + \mathbf{k}_{2T} = \vec{\cancel{p}}_T} [\max \{M_T(\mathbf{p}_{1T}, \mathbf{p}_{2T}), M_T(\mathbf{k}_{1T}, \mathbf{k}_{2T})\}] \quad (16)$$

where M_T is the transverse mass

$$M_T^2(\mathbf{p}_{1T}, \mathbf{p}_{2T}) = 2(|\mathbf{p}_{1T}||\mathbf{p}_{2T}| - \mathbf{p}_{1T} \cdot \mathbf{p}_{2T}) . \quad (17)$$

For an event without initial state radiation the transverse MAOS momenta are simply given by

$$\mathbf{p}_{2T}^{\text{maos}} = -\mathbf{k}_{1T}, \quad \mathbf{k}_{2T}^{\text{maos}} = -\mathbf{p}_{1T}. \quad (18)$$

There can be two different schemes to define the longitudinal MAOS momenta. One is to require the on-shell conditions for both the invisible particles in the final state and the mother particles in the intermediate state (W) [13] (here called MAOS-original) which results into a four-fold degeneracy

$$\begin{aligned} p_{2L}^{\text{maos}}(\pm) &= \frac{1}{|\mathbf{p}_{1T}|^2} [p_{1L} A \\ &\pm \sqrt{|\mathbf{p}_{1T}|^2 + p_{1L}^2} \sqrt{A^2 - |\mathbf{p}_{1T}|^2 |\mathbf{p}_{2T}^{\text{maos}}|^2}] , \\ k_{2L}^{\text{maos}}(\pm) &= \frac{1}{|\mathbf{k}_{1T}|^2} [k_{1L} B \\ &\pm \sqrt{|\mathbf{k}_{1T}|^2 + k_{1L}^2} \sqrt{B^2 - |\mathbf{k}_{1T}|^2 |\mathbf{k}_{2T}^{\text{maos}}|^2}] , \end{aligned} \quad (19)$$

where $A \equiv M_{Z'}^2/2 + \mathbf{p}_{1T} \cdot \mathbf{p}_{2T}^{\text{maos}}$ and $B \equiv M_{Z'}^2/2 + \mathbf{k}_{1T} \cdot \mathbf{k}_{2T}^{\text{maos}}$.

Another possible scheme [18] is to require

$$\begin{aligned} (p_2^{\text{maos}})^2 &= (k_2^{\text{maos}})^2 = 0 , \\ (p_1 + p_2^{\text{maos}})^2 &= (k_1 + k_2^{\text{maos}})^2 = M_{Z'}^2 , \end{aligned} \quad (20)$$

which gives unique longitudinal MAOS momenta (here called MAOS-modified) as

$$p_{2L}^{\text{maos}} = \frac{|\mathbf{p}_{2T}^{\text{maos}}|}{|\mathbf{p}_{1T}|} p_{1L}, \quad k_{2L}^{\text{maos}} = \frac{|\mathbf{k}_{2T}^{\text{maos}}|}{|\mathbf{k}_{1T}|} k_{1L}. \quad (21)$$

To illustrate the accuracy of the neutrino momenta determination in the MAOS reconstruction we present in Fig. 6 the reconstructed $Z' \rightarrow W^+W^-$ invariant mass using the MAOS-original (with sign ++ in Eq. (19) for illustration), MAOS-modified (21), and the WW transverse invariant mass (15). For the sake of comparison the shaded (green) area represents the actual spectrum. As we can see, the three methods lead to similar results which is expected since the signal is dominated by Z' decaying into on-shell W 's. Furthermore, in all cases the characteristic peak associated with the production of the resonance is substantially broadened. However it is still possible to suppress the backgrounds and enhance the Z' signal by demanding that any of the reconstructed WW masses to be around $M_{Z'}$ within a broad width.

Consequently in our study we demand the WW transverse invariant mass to comply with

$$M_T^{WW} > \frac{M_{Z'}}{2} , \quad (22)$$

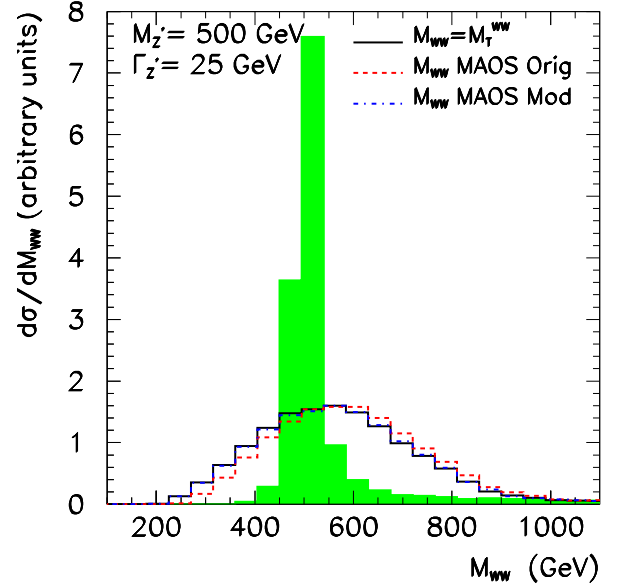


FIG. 6: Reconstructed WW invariant mass distributions for $pp \rightarrow Z' \rightarrow W^+W^- \rightarrow \ell^- \ell^+ \cancel{E}_T$ assuming $M_{Z'} = 500$ GeV and $\Gamma_{Z'} = 25$ GeV. The solid (black) line corresponds to $M_{WW} = M_T^{WW}$ (15). The dashed (red) line stands for the invariant mass reconstructed using the MAOS-original momentum prescription with sign ++ in Eq. (19) and the dash-dot (blue) line represents MAOS-modified (21) prescription. The shadow (green) area represents the true spectrum.

where only a lower cut is required because the background is a very steeply falling function of M_T^{WW} .

After the cuts (14) and (22), the $t\bar{t}$ SM background is still quite large, therefore we veto the presence of additional jets in the event with

$$|\eta_j| < 3 \quad \text{and} \quad p_T^j > 20 \text{ GeV}. \quad (23)$$

However, QCD radiation and pile-up can lead to the appearance of an additional jet even in signal events. Therefore, we must introduce the probability of a QCD (electroweak) event to survive such a central jet veto [19]. The survival probability due to pile-up has been estimated to be 0.75 for a threshold cut of $p_T = 20$ GeV in Ref. [20]. Taking into account these two effects we included in our analysis veto survival probabilities

$$P_{\text{surv}}^{\text{EW}} = 0.56 \quad , \quad P_{\text{surv}}^{\text{QCD}} = 0.23 . \quad (24)$$

For events presenting same flavor lepton pairs, *i.e.* ee or $\mu\mu$, there is an additional SM contribution stemming from ZZ production with one of the Z decaying invisibly and the other into a charged lepton pair. For these final states, we supplement the cuts (14), (22), and (23) further imposing that

$$\cancel{E}_T > 50 \text{ GeV} \quad \text{and} \quad m_{\ell^+ \ell^-} > 100 \text{ GeV}. \quad (25)$$

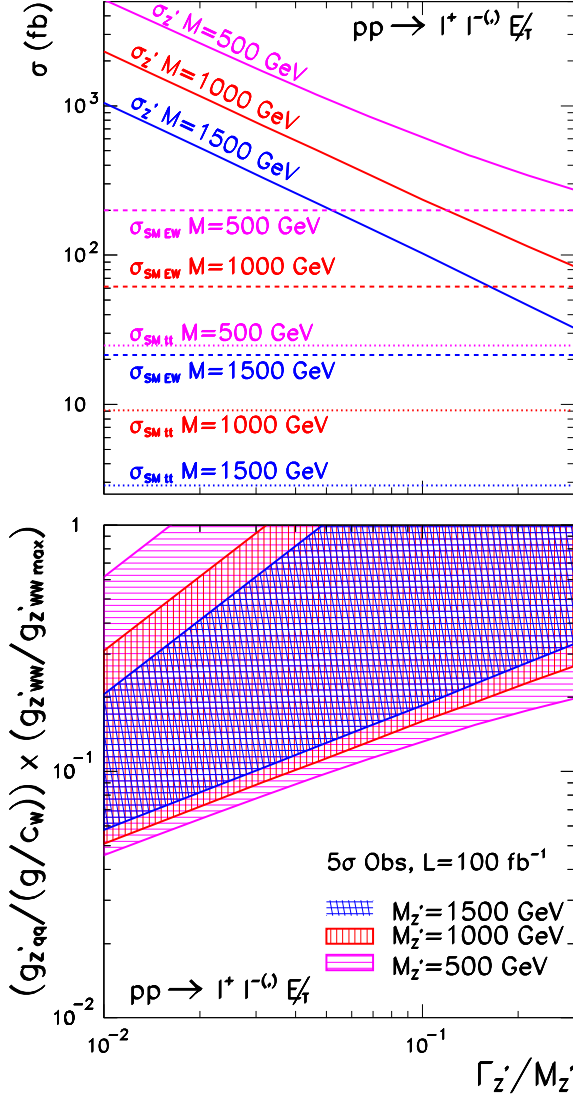


FIG. 7: **Upper panel:** signal and background cross sections for the $\ell^+ \ell'^- \cancel{E}_T$ final state for all possible lepton flavor combinations without including lepton detection efficiencies nor survival probabilities. **Lower panel:** the filled regions are the ranges of the parameters for observation of a W' with mass $M_{W'} = 0.5, 1, \text{ and } 1.5$ TeV with at least 5σ significance in the reaction $pp \rightarrow Z' \rightarrow W^+ W^- \rightarrow \ell^+ \ell'^- \cancel{E}_T$ for an integrated luminosity of 100 fb^{-1} .

We denote the sum of the SM backgrounds not originating from $t\bar{t}$ production as EW background.

We show in the upper panel of Fig. 7 the values of $\sigma_{Z'}$ and σ_{SM} for the electroweak and $t\bar{t}$ backgrounds at $\sqrt{s} = 14$ TeV. Once the cuts described above are imposed the interference term is negligible for all values of Z' masses and widths considered. We see that the backgrounds for Z' in the leptonic final states are considerably larger than the ones for W' as a consequence of the very broad re-

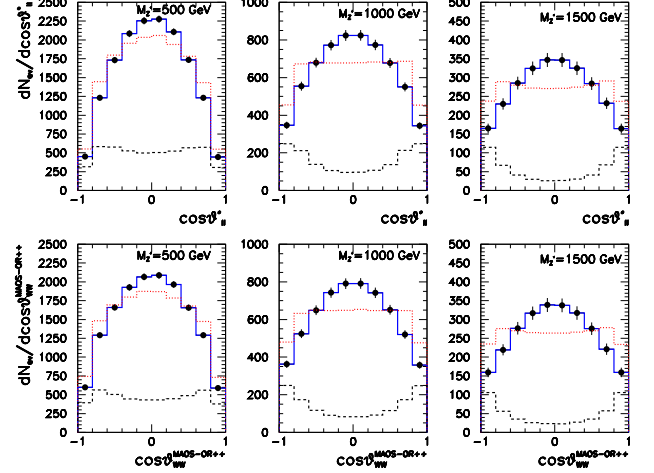


FIG. 8: $\cos \theta_{ll}^*$ (upper panels) and $\cos \theta_{WW}^{\text{MAOS-OR++}}$ (lower panels) distributions for the production of the neutral vector resonance (solid blue line with error bars), and the production of a neutral scalar resonance (dotted red line). The results are shown for $\Gamma_{Z'} = 0.01 M_{Z'}$ and $\left(\frac{g_{Z'q\bar{q}}}{g_{Zq\bar{q}}} \frac{g_{Z'WW}}{g_{Z'WW_{\max}}} \right) = 0.3$. The contribution of the SM background is depicted by the dashed black line. We assumed an integrated luminosity of 100 fb^{-1} .

construction of the Z' invariant mass in this channel. For the sake of completeness we depict in the lower panel of Fig. 7 the parameter space region where the LHC will be able to observe a Z' with at least 5σ significance level for an integrated luminosity of 100 fb^{-1} . For this luminosity the number of background events is always large enough for Gaussian statistics to hold and we impose $N_{Z'} \geq 5\sqrt{N_{SM}}$, where $N_{Z'} = \mathcal{L} \times \sigma_{Z'} \times P_{\text{surv}}^{\text{EW}} \times (\epsilon^\ell)^2$ and $N_{SM} = \mathcal{L} \times (\sigma_{SM}^{\text{EW}} \times P_{\text{surv}}^{\text{EW}} + \sigma_{SM}^{t\bar{t}} \times P_{\text{QCD}}) \times (\epsilon^\ell)^2$. Comparing with Fig. 1 we find that establishing the existence of a Z' requires larger couplings to light quark and vector boson pairs than a W' as a consequence of the larger SM backgrounds.

Nowadays, a small part of the lower panel of Fig. 7 has been directly probed. The CDF analysis [16] indicates that for narrow 500 GeV Z' 's

$$\left(\frac{g_{Z'q\bar{q}}}{g_{Zq\bar{q}}} \times \frac{g_{Z'WW}}{g_{Z'WW_{\max}}} \right) \gtrsim 0.19$$

is excluded at 95% CL.

In order to discriminate the spin of the neutral resonance we first employ the variable $\cos \theta_{\ell\ell}^*$ (11) using the two opposite charge leptons which does not require the determination of the neutrino momenta, therefore avoiding reconstruction ambiguities. We plot in Fig. 8 (upper panels) the $\cos \theta_{\ell\ell}^*$ spectrum for the production of spin-0 and spin-1 resonances for our three reference masses and assuming a width of $\Gamma_{Z'} = 0.01 M_{Z'}$ and $\left(\frac{g_{Z'q\bar{q}}}{g_{Zq\bar{q}}} \frac{g_{Z'WW}}{g_{Z'WW_{\max}}} \right) = 0.3$. We imposed that the spin-0

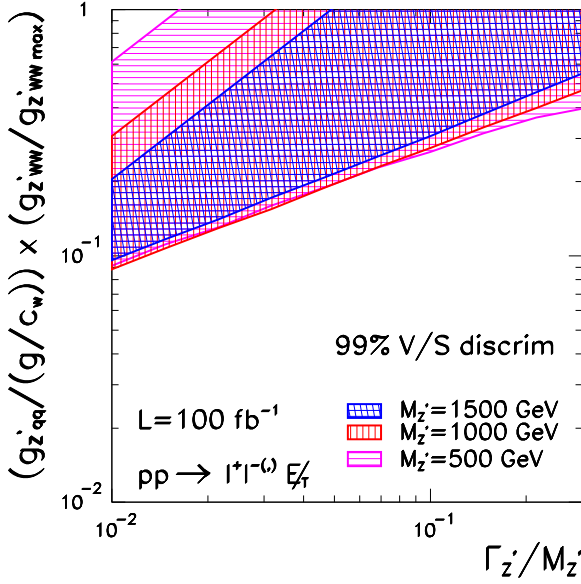


FIG. 9: Parameter space region where the Z' spin determination can be done at 99% CL for an integrated luminosity for 100 fb^{-1} using the asymmetry $A_{\ell\ell}$.

production cross section has the spin-1 value. Analogously to the W' case, we can see that the acceptance cuts distort considerably the spin-0 spectrum at lower masses. For heavier states the final state leptons have a larger tendency to follow the direction of the parent W since it is more energetic, ameliorating the effect of the cuts. Another important feature of this case is that the SM background is no longer negligible.

We have also explored the expected distribution of the W polar angle in the W^+W^- center-of-mass frame as reconstructed using the different MAOS prescriptions. As an illustration we depict, in the lower panels of Fig. 8, the reconstructed $\cos\theta_{WW}$ spectrum for the production of spin-0 and spin-1 resonances and our three reference masses as obtained from the MAOS-original momentum prescription with sign $++$ in Eq. (19). The comparison of the distributions of the two angular variables presented in this figure indicates that these variables are correlated. Indeed they are strongly correlated as can be seen in the lower panels of Fig. 3. Consequently, as in the W' case, we can foresee a similar spin discriminating power for both variables on the basis of statistics. We have verified that the same conclusion is reached when using either the MAOS-original momentum prescription with sign $--$ in Eq. (19), the average of the distributions with $+-$ and $-+$ signs, or the MAOS-modified prescription (21).

We present in Fig. 9 the Z' parameter space region where the LHC can establish its spin with 99% CL using $A_{\ell\ell}$ for an integrated luminosity of 100 fb^{-1} . As in the W' case, the minimum couplings needed for the spin

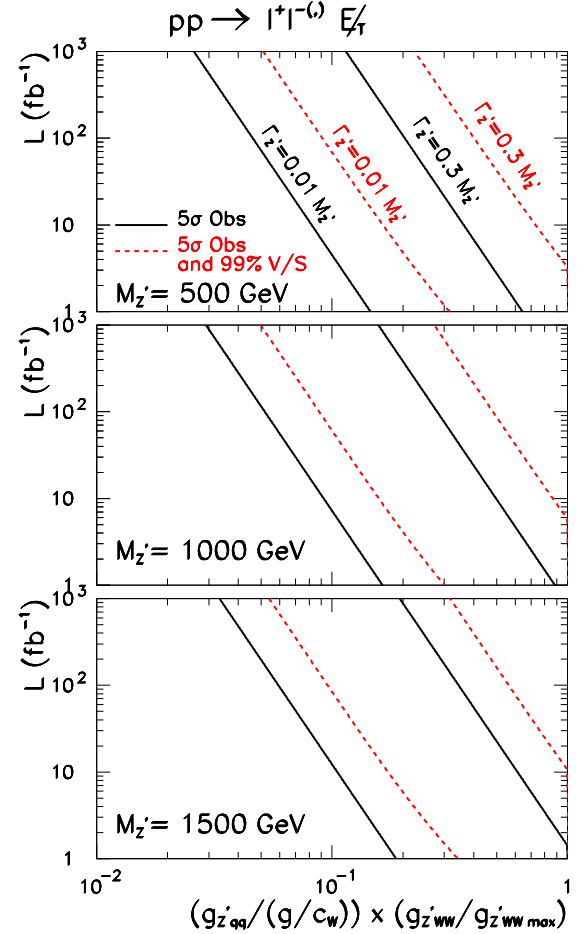


FIG. 10: The solid (dashed) lines stand for integrated luminosity required for the 5σ discovery (99% CL spin determination) as a function of the vector resonance couplings. We present the results for three masses and two widths: $\Gamma_{Z'} = 0.01 M_{Z'}$ and $\Gamma_{Z'} = 0.3 M_{Z'}$.

determination are approximated twice the ones required for the Z' discovery. Moreover, the minimum couplings required for the spin determination exhibit a very mild dependence on the resonance mass since the acceptance cut effects are smaller for heavier states, compensating, partially, the decrease in the production cross section.

Finally we show in Fig. 10 the required integrated luminosity for a 5σ discovery (solid lines) and 99% CL spin determination based on (13) (dashed lines) for our three reference masses and two widths ($\Gamma_{Z'} = 0.01 M_{Z'}$ and $\Gamma_{Z'} = 0.3 M_{Z'}$) as a function of the Z' couplings. We find that for a given value of the Z' couplings the required luminosity for 99% CL spin determination based on the study of $A_{\ell\ell}$ is a factor ~ 20 (10) {9} larger than the one required for 5σ discovery for $M_{Z'} = 500$ (1000) {1500} GeV and that these factors are almost independent of $\Gamma_{Z'}/M_{Z'}$.

V. SUMMARY

In this work we have performed a model independent analysis of the LHC potential to unravel the spin of new charged and neutral vector resonances associated with the EWSB sector that are predicted in many extensions of the SM. The production of a charged vector resonance leads to trilepton final states and we showed that the study of the $\cos\theta_{\ell\ell}^*$ and the reconstructed $\cos\theta_{WZ}$ distributions yield similar discriminating power for the spin of the new state. We find that the study of the trilepton channel can lead to a 99% CL determination of the new charged state spin in a large fraction of the parameter space where this state can be observed at the LHC for an integrated luminosity of 100 fb^{-1} . As an illustration, let us consider the case of Higgsless models [3] where the W' mass is expected to be lighter than 1 TeV and that

$$\left(\frac{g_{W'q\bar{q}}}{g_{Wq\bar{q}}} \frac{g_{W'WZ}}{g_{W'WZ_{max}}} \right) \simeq \mathcal{O}(0.07) .$$

The range of these parameters indicates that this new state should be observed with an integrated luminosity of the order of 10 fb^{-1} , while the determination of its spin should require a few tens fb^{-1} .

The analyses for the neutral spin-1 resonances was carried out using the production of opposite charge dileptons. It turns out that the SM background in this case can be efficiently reduced, however, it is not completely eliminated by the cuts, consequently leading to a larger required luminosity for the discovery and determination of the spin of the neutral new particles. We considered two methods for the reconstruction of the final state neutrinos (and consequently of the Z' mass) MAOS-original

and MAOS-modified, that lead to similar results. We find that the variables $\cos\theta_{\ell\ell}^*$ and $\cos\theta_{WW}$ with $\cos\theta_{WW}$ reconstructed with any of the MAOS methods lead to equivalent precision in the spin determination of the Z' . Analogously to the W' case, the 99% CL determination of the neutral resonance spin can be carried out in a large fraction of the discovery parameter space for a fixed integrated luminosity. In the particular case of Higgsless models [3], the Z' mass is expected to be smaller than 1 TeV and its couplings

$$\left(\frac{g_{Z'q\bar{q}}}{g_{Zq\bar{q}}} \frac{g_{Z'WW}}{g_{Z'WW_{max}}} \right) \simeq \mathcal{O}(0.1)$$

which implies that an integrated luminosity of 100 fb^{-1} should be enough for a Z' discovery and to unravel its spin.

Acknowledgments

We would like to thank E.G. Moraes and P.G. Mercadante for enlightening discussions. O.J.P.E is supported in part by Conselho Nacional de Desenvolvimento Científico e Tecnológico (CNPq) and by Fundação de Amparo à Pesquisa do Estado de São Paulo (FAPESP); M.C.G-G is also supported by USA-NSF grant PHY-0969739 and by Spanish grants from INFN-MICINN agreement program ACI2009-1038, consolidator-ingénio 2010 program CSD-2008-0037, by CUR Generalitat de Catalunya grant 2009SGR502 and together with J.G-F by MICINN 2007-66665-C02-01. J.G-F is further supported by Spanish ME FPU grant AP2009-2546.

-
- [1] B. W. Lee, C. Quigg, and H. B. Thacker, Phys. Rev. Lett. **38**, 883 (1977).
 - [2] B. W. Lee, C. Quigg, and H. B. Thacker, Phys. Rev. D **16**, 1519 (1977).
 - [3] C. Csaki, C. Grojean, H. Murayama, L. Pilo, and J. Terning, Phys. Rev. D **69**, 055006 (2004) [arXiv:hep-ph/0305237]; C. Csaki, C. Grojean, L. Pilo, and J. Terning, Phys. Rev. Lett. **92**, 101802 (2004) [arXiv:hep-ph/0308038]; G. Cacciapaglia, C. Csaki, C. Grojean, and J. Terning, Phys. Rev. D **70**, 075014 (2004) [arXiv:hep-ph/0401160]; G. Cacciapaglia, C. Csaki, G. Marandella, and J. Terning, Phys. Rev. D **75**, 015003 (2007) [arXiv:hep-ph/0607146]; Y. Nomura, J. High Energy Phys. **0311**, 050 (2003) [arXiv:hep-ph/0309189]; R. S. Chivukula, D. A. Dicus, H. -J. He, Phys. Lett. **B525**, 175-182 (2002). [hep-ph/0111016]; R. S. Chivukula, H. -J. He, Phys. Lett. **B532**, 121-128 (2002). [hep-ph/0201164].
 - [4] S. Dimopoulos and L. Susskind, Nucl. Phys. B **155**, 237 (1979); L. Susskind, Phys. Rev. D **20**, 2619 (1979); S. Weinberg, Phys. Rev. D **19**, 1277 (1979).
 - [5] See for instance, C. T. Hill and E. H. Simmons, Phys. Rept. **381**, 235 (2003) [Erratum-ibid. **390**, 553 (2004)] [arXiv:hep-ph/0203079];
 - [6] A. Birkedal, K. Matchev, and M. Perelstein, Phys. Rev. Lett. **94**, 191803 (2005) [arXiv:hep-ph/0412278].
 - [7] A. Alves, O. J. P. Eboli, M. C. Gonzalez-Garcia *et al.*, Phys. Rev. D **79**, 035009 (2009). [arXiv:0810.1952 [hep-ph]].
 - [8] The Z' leptonic decay can be observed in its associated production with a hadronically decaying W , see M. Asano, Y. Shimizu, JHEP **1101**, 124 (2011). [arXiv:1010.5230 [hep-ph]].
 - [9] A. J. Barr, Phys. Lett. B **596**, 205 (2004) [arXiv:hep-ph/0405052]. A. J. Barr, J. High Energy Phys. **0602**, 042 (2006) [arXiv:hep-ph/0511115].
 - [10] J. M. Smillie and B. R. Webber, J. High Energy Phys. **0510**, 069 (2005), [arXiv:hep-ph/0507170]; A. Alves, O. Éboli, and T. Plehn, Phys. Rev. D **74**, 095010 (2006) [arXiv:hep-ph/0605067]; A. Alves and O. Éboli, Phys. Rev. D **75**, 115013 (2007) [arXiv:0704.0254 [hep-ph]].
 - [11] R. Cousins, J. Mumford, J. Tucker *et al.*, JHEP **0511**, 046 (2005); Y. Gao, Y. Gao, A. V. Gritsan, Z. Guo *et al.*, Phys. Rev. D **81**, 075022 (2010).

- [arXiv:1001.3396 [hep-ph]]; C. Englert, C. Hackstein, M. Spannowsky, Phys. Rev. **D82**, 114024 (2010). [arXiv:1010.0676 [hep-ph]]; M. R. Buckley, H. Murayama, W. Klemm, and V. Rentala, Phys. Rev. D **78**, 014028 (2008) [arXiv:0711.0364 [hep-ph]]; L. T. Wang and I. Yavin, JHEP **0704**, 032 (2007) [arXiv:hep-ph/0605296]; L. Edelhauser, W. Porod, R. K. Singh, JHEP **1008**, 053 (2010). [arXiv:1005.3720 [hep-ph]]; W. Ehrenfeld, A. Freitas, A. Landwehr *et al.*, JHEP **0907**, 056 (2009). [arXiv:0904.1293 [hep-ph]]; F. Boudjema, R. K. Singh, JHEP **0907**, 028 (2009). [arXiv:0903.4705 [hep-ph]]; O. Gedalia, S. J. Lee, G. Perez, Phys. Rev. **D80**, 035012 (2009). [arXiv:0901.4438 [hep-ph]]; L. -T. Wang, I. Yavin, Int. J. Mod. Phys. **A23**, 4647-4668 (2008). [arXiv:0802.2726 [hep-ph]].
- [12] A. Alves, O. J. P. Eboli, D. Goncalves *et al.*, Phys. Rev. **D80**, 073011 (2009). [arXiv:0907.2915 [hep-ph]].
- [13] W. S. Cho, K. Choi, Y. G. Kim *et al.*, Phys. Rev. **D79**, 031701 (2009). [arXiv:0810.4853 [hep-ph]].
- [14] T. Stelzer and F. Long, Comput. Phys. Commun. **81** (1994) 357; F. Maltoni and T. Stelzer, J. High Energy Phys. **0302**, 027 (2003) [arXiv:hep-ph/0208156].
- [15] J. Pumplin, D. R. Stump, J. Huston, H. L. Lai, P. Nadolsky and W. K. Tung, JHEP **0207**, 012 (2002) [arXiv:hep-ph/0201195].
- [16] T. Aaltonen *et al.* [The CDF Collaboration], Phys. Rev. Lett. **104**, 241801 (2010). [arXiv:1004.4946 [hep-ex]].
- [17] C. G. Lester, D. J. Summers, Phys. Lett. **B463**, 99-103 (1999). [hep-ph/9906349].
- [18] K. Choi, S. Choi, J. S. Lee *et al.*, Phys. Rev. **D80**, 073010 (2009). [arXiv:0908.0079 [hep-ph]].
- [19] D. Rainwater, Ph.D. thesis, report arXiv:hep-ph/9908378.
- [20] V. Cavasinni, D. Costanzo and I. Vivarelli, ATL-PHYS-2002-008; S. Asai *et al.*, Eur. Phys. J. C **32S2**, 19 (2004).